Available online at www.sciencedirect.com

ScienceDirect

Procedia Engineering 00 (2017) 000–000

Procedia Engineering

www.elsevier.com/locate/procedia

International Conference on the Technology of Plasticity, ICTP 2017, 17-22 September 2017, Cambridge, United Kingdom

Dry friction during sliding of AA1050 on AA2024 at elevated temperature.

Hubert Geijselaers[a]*, Arnoud van der Stelt[b], Ton Bor[a]

[a]*University of Twente, POBox 217, 7500 AE Enschede, the Netherlands*
[b]*Demcon-Bunova, Institutenweg 25, 7521 PH Enschede, the Netherlands*

Abstract

The friction development between Aluminium AA1050 and Dural AA2024 is studied. Continuous full surface rotational sliding experiments of AA1050 over AA2024 were performed at temperatures between 150 and 350 °C and at contact pressures between 2 and 15 MPa. The required torque was measured as function of rotation angle.
A model is set up for the evolution of the friction coefficient, which takes into account temperature, normal pressure and sliding distance. Validation of the model is done by implementation in a finite element program and reproduction of observed behaviour.

Peer-review under responsibility of the scientific committee of the International Conference on the Technology of Plasticity.
Keywords: Friction; solid bonding; friction surfacing; friction stir cladding

1. Introduction

The shear stress due to friction at the interface of two contacting bodies is generally described by Coulomb's law. It relates the value of the shear stress τ during sliding to the applied pressure p by a friction coefficient μ: $\tau = \mu p$. For AA6061 sliding on AA6061 values for static and dynamic friction coefficients in air at room temperature were quoted as 0.42 and 0.34 [1–3]. For aluminium sliding on aluminium plate a static friction coefficient was measured of 0.57 [1–3]. For clean 99% pure aluminium in helium gas static friction coefficients of 1.62 and 1.60 at respectively 80K

* Corresponding author. Tel.: +31-53-4892443.
E-mail address: h.j.m.geijselaers@utwente.nl

Peer-review under responsibility of the scientific committee of the International Conference on the Technology of Plasticity.

and 300K have been reported [2]. Other values for the static friction coefficient of 1.05 and 1.9 [2] and 1.35 [4] were presented. The large variation in reported friction coefficients indicates that a constant friction coefficient is not applicable to describe the friction of aluminum sliding on aluminum.

At high contact pressures the shear stress depends on the material's shear strength τ_y, rather than on the pressure. Tresca related the friction to the material's shear strength through a friction factor m: $\tau = m\tau_y$. A combination of the Coulomb and Tresca models was suggested by Orowan [5]. Wanheim and Bay introduced a friction model for metal forming which provides a smooth transition between a friction model with a constant Coulomb's friction coefficient at low forming loads and a friction factor model which depends on the material strength at high loads [6,7].

When two objects slide with respect to each other, this changes the interface conditions. The coefficient of friction will not remain constant. In this contribution we report on evolution of friction during continuous sliding experiments of pure aluminum on AA2024. This is in contrast to experiments and models, which deal with friction during initial or intermittent sliding. A model will be derived and by a finite element simulation of the experiments its applicability will be shown.

2. Experimental setup

Experiments were performed on a torsion friction tester [8,9]. The setup was adapted as shown in Figure 1(a) to perform sliding friction experiments. An AA1050-O disc is positioned between two AA2024-T351 parts. A steel pin keeps the three parts aligned and the two steel blocks are connected to the friction tester. The parts are compressed and heated. Subsequently, a rotation is applied to the lower steel block while the upper steel block remains fixed. The stationary upper part contains 2 thermocouples located at opposite sides of the center line at a radius of 8 mm and at 2.4 mm above the surface that is in contact with the AA1050 disc, see Figure 2(c). A rotation speed of 10 rpm (≈1 rad/s) is used during the experiments. In this setup the aluminium slides continuously over the same surface. In this way the oxide layer at the AA1050/AA2024 interfaces gradually breaks up and eventually both materials will bond.

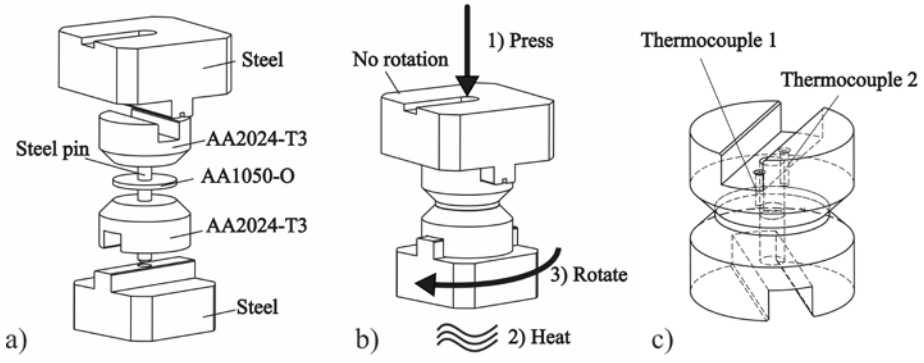

Fig. 1. The experimental setup: (a) assembly; (b) experiment; (c) thermocouple locations.

The AA1050 discs were produced from a 2.0 mm thick rolled plate from which circular discs with a radius of 14 mm were cut. The AA2024 parts were machined from rod. The surface contacting the AA1050 in the experiment was milled with a tolerance of 0.01 mm for its flatness and with a roughness value between 0.8 and 1.6 R_a (μm).

Each experiment started by removing the protective foils from both sides of the AA1050 disc and by cleaning all aluminium parts with ethanol. Next, the parts were assembled and a normal load was applied to the setup, see Figure 2(b). The sample was heated till it reached a temperature of 10 °C above the required temperature of the experiment. The sample was let to cool down after switching off the heater and as soon as the desired temperature was reached, a rotation angle Θ was applied. The torque, displacement in axial direction, temperature and normal force were recorded.

The temperature at the interface rises during the experiment as a result of the heat produced by friction. Based on applied work and taking heat conduction into account, the temperature rise near the interface is estimated at 7 °C per half a revolution (i.e. 180°) at the outer radius of the interface. The order of magnitude of the temperature rise is confirmed by readings of the thermocouples during the experiments.

3. Model of the shear stress at the interface

The stress in the aluminium disc is a combined shear and pressure. At low pressure there will be slip at the interface, at high pressures, the whole disc may yield while torqued. Below the yield strength of the disc the maximum shear stress is determined by Coulombs law:

$$\tau_{\max} = \mu p\,. \tag{1}$$

The friction coefficient at the start of the experiment is μ_0. It corresponds to a friction coefficient for an interface that has not significantly been deformed and where no bonding has yet occurred. The shear stress corresponding to $\mu_0 p$ is plotted in figure 2a as a solid straight line. During the experiment a gradual increase of the friction coefficient is expected, which is indicated by a bundle of dashed straight lines.

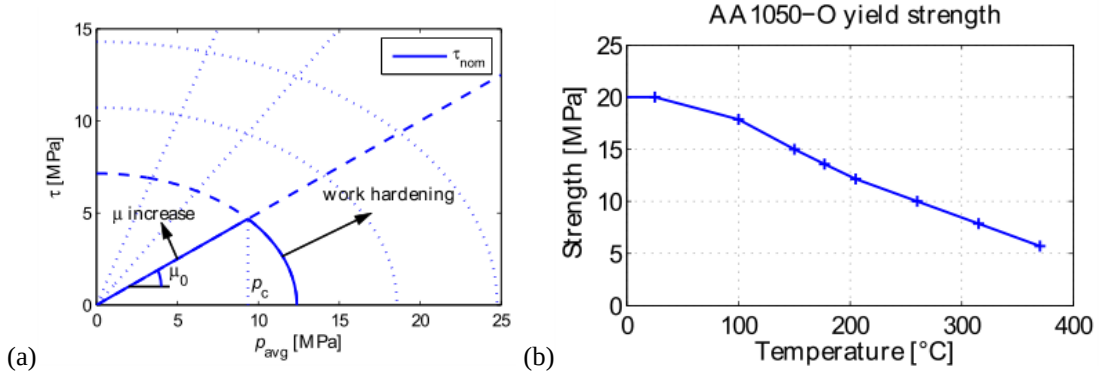

(a) (b)

Fig. 2. (a) Evolution of the expected nominal shear stress τ_{nom}; (b) the yield strength of AA 1050-O as function of temperature [10].

The onset of plastic deformation is determined by the von Mises yield criterion:

$$\tau = \sqrt{(\sigma_y^2 - p^2)/3}\,, \tag{2}$$

where σ_y is the yield strength of the AA1050. This is indicated by the ellipse in figure 2a. When deformation occurs, the yield stress will rise due to hardening. This is also shown in figure 2a by a series of concentric dashed ellipses. After some time during a test the shear stress is assumed to be determined by the intersection of the Coulomb friction line and the yield ellipse. Of both of these the level increases due to sliding at the interface as well as plastic hardening of the AA1050 specimen.

4. Experimental results

At a temperature of 200 °C a wide range of experiments with different applied pressures and different applied rotation angles was performed. Of two representative settings torque vs. rotation angle plots are shown in figure 3. More experiments were performed at T = 150, 250, 300 and 350 °C.

By visual inspection, of each specimen can be determined whether it has plastically deformed or not. The results for T = 200 °C are presented in figure 3c. Here also both the yield envelope and the initial friction cone with μ_0 = 0.5 are plotted. The model as presented in Section 3 appears valid.

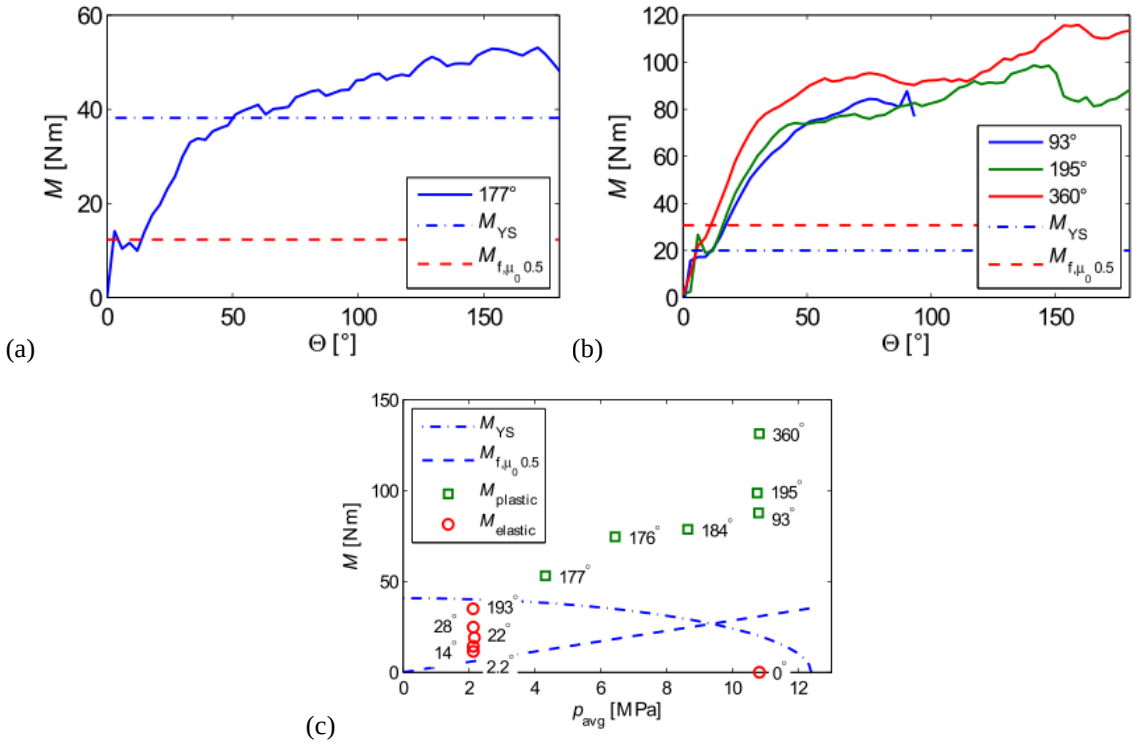

Fig. 3. Experimental results at T = 200 °; (a) torque vs. angle at applied pressure p = 4.3 MPa; (b) torque vs. angle at p = 10.8 MPa. M_{YS} is the toque required for yielding, whereas M_f is the torque to overcome friction; (c) maximum measured torques for all applied pressures and rotation angles. Squares indicate plastically deformed samples.

5. Evolution of the friction coefficient

The development of the shear stress at the interface, as function of the rotation θ, is measured through the torque:

$$M(\theta) = \int_{R_i}^{R_o} 2\pi r^2 \tau(r,\theta)\,\mathrm{d}\,r\,. \tag{3}$$

When sliding occurs, the interface deforms due to ploughing, which results in a strong increase of the shear stress [11]. Therefor the shear stress is assumed as a function of pressure p, temperature T and sliding distance s:

$$\frac{\tau}{\tau_y(T)} = b\left(\frac{p}{\sigma_y(T)}\right)^n \exp\left(\frac{-Q}{RT}\right)\left(1-\exp\left(-\frac{s}{L}\right)\right), \tag{4}$$

where parameter b is a constant and L a reference sliding length. The term p/σ_y is a measure for the asperity flattening at the interface. The term describing dependence on sliding distance follows from deconvolution of the torque signal (figure 3) [12], which indicates that the dependence on sliding distance saturates. The Arrhenius thermal activation Q is included since diffusion-like phenomena are expected to play a role in interface bonding.

For application of the model to circumstances of varying pressure and temperature, Eq. (4) is written as a rate equation for the coefficient of friction μ_s due to sliding as it irreversibly evolves:

$$\dot{\mu}_s = \left\langle \frac{b}{\sqrt{3}} \left(\frac{p}{\sigma_y} \right)^{n-1} e^{\frac{-Q}{RT}} - \mu_s \right\rangle \frac{\dot{s}}{L}, \tag{5}$$

The parameters b, n, Q and L of the friction model have been fitted to the results of the tests performed at T = 150, 200 and 250 °C, using an analytical solution of Eq. (3), assuming constant pressure. The numerical values are given in Table 1. The fitted value for the activation energy appears to be unrealistically low. This indicates, that probably diffusion doesn't play a role. However for a proper fit a temperature dependence in addition to that of the yield stress is required.

Table 1. Parameters of the friction model Eq. (4) fitted from experiments.

Parameter	b	n	Q	L
value	25	0.67	9100 J/mol	0.002 m

6. Finite Element implementation

To verify whether the fitted values also apply when plastic deformation of the test specimens occurs, the model has been implemented as an evolving friction law in contact elements of an in-house ALE finite element code [13,14]. The coefficient of friction is determined as $\mu = \max(\mu_0, \mu_s)$, where μ_0 is the initial coefficient and μ_s is the coefficient of friction as it evolves according to Eq. (5). The used values of μ_0 are summarized in Table 2.

Table 2. Initial coefficient of friction values used in the finite element model.

Temperature	150 °C	200 °C	250 °C	300 °C	350 °C
Initial coefficient of friction μ_0	0.3	0.5	0.6	1.0	1.0

The AA2024 parts are modeled with elastic behavior. The AA1050 disk is modeled with elasto-plastic material behavior with von-Mises yielding and Voce hardening with a saturation flow stress of 3 times the initial yield stress:

$$\sigma_y(\varepsilon_{eq}) = \sigma_y + 2\sigma_y(1 - \exp(-\varepsilon_{eq} / 0.01)), \tag{6}$$

based on data from [15,16]. Temperature dependence of the AA1050 yield stress is shown in figure 2b.

6.1. Results

The torque vs. rotation results of the simulations are plotted together with experimental results for all experiments in figure 4. Overall they have a reasonable correspondence. After an initial small elastic deformation, sliding starts with initial coefficient of friction μ_0. Due to sliding, gradually the evolving sliding friction coefficient μ_s increases from outer radius inwards to a level above the initial one. Finally the friction becomes high enough to induce massive yielding of the disk.

7. Conclusions

In this contribution we show results from continuous sliding experiments of AA1050 on AA2024. A model for continuous sliding friction has been assumed and parameters for this model have been obtained by fitting to experiments. Finite element simulations with this model implemented in a contact element render the experimental results.

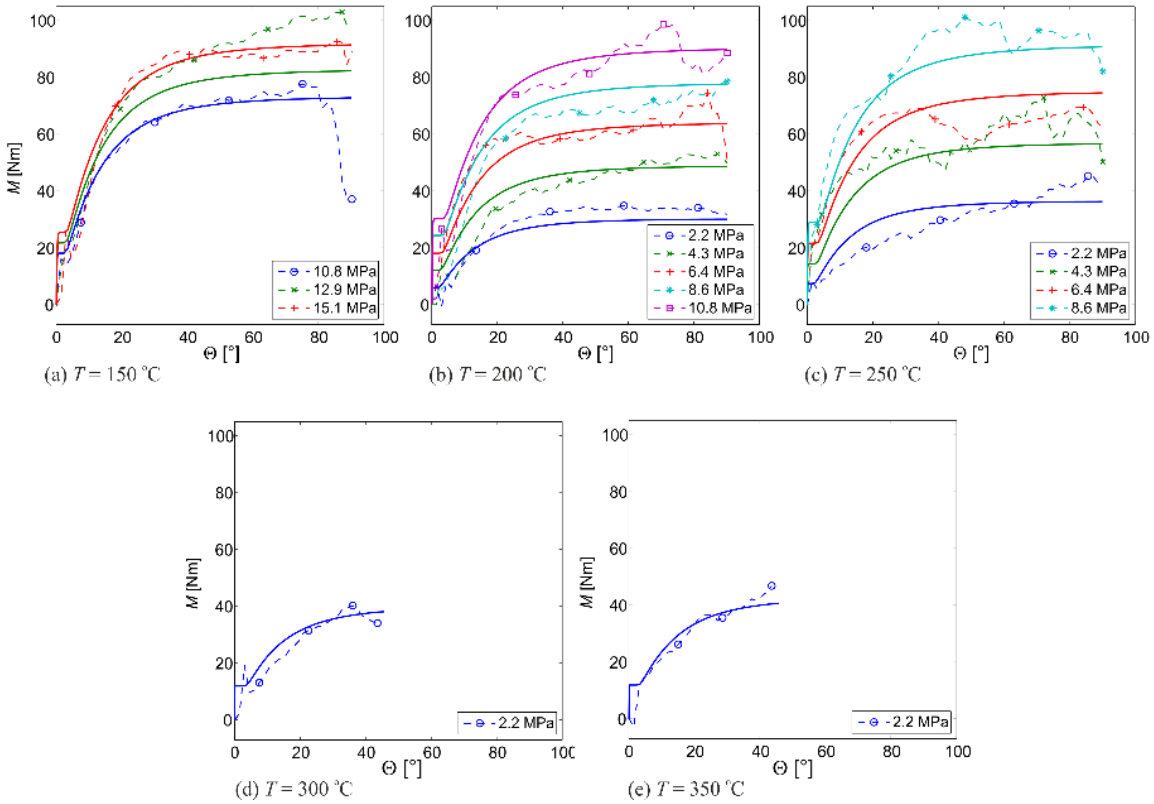

Fig. 4. Torque vs. rotation angle, experimental and finite element model results at different temperatures and applied pressures.

References

[1] P.J. Blau (Ed.), ASM Handbook Volume 18: Friction, Lubrication, and Wear Technology. ASM International, OH, USA, 1992.
[2] P.J. Blau. Friction Science and Technology. CRC Press, FL, USA, 2nd edition, 2008.
[3] J.R. Davis. Concise Metals Engineering Data Book. ASM International, OH, USA, 1997.
[4] E. Oberg, F.D. Jones, H.L. Horton. Machinery's Handbook: A Reference Book for the Mechanical Engineer, Designer, Manufacturing Engineer, Draftsman, Toolmaker, and Machinist. Industrial Press, NY, USA, 24th edition, 1997.
[5] E. Orowan. The calculation of roll pressure in hot and cold flat rolling. Proc. Inst. Mech. Eng. 150 (1943) 140-167.
[6] T. Wanheim, N. Bay. A model for friction in metal forming processes. CIRP Ann.-Manuf. Techn. 27 (1978) 189-194.
[7] P.M. Dixit, U.S. Dixit. Modeling of metal forming and machining processes. Springer-Verlag, London, UK, 2008.
[8] F.Widerøe, T.Welo. Conditions for sticking friction between aluminium alloy AA6060 and tool steel in hot forming. Key Eng. Mat. 491 (2011) 121-128.
[9] F.Widerøe, T.Welo, H. Vestøl. A new testing machine to determine the behaviour of aluminium granulate under combined pressure and shear. Int. J. of Mat. Form. 6 (2013) 199-208, 2013.
[10] J.G. Kaufman. Properties of Aluminum Alloys: Tensile, Creep, and Fatigue Data at High and Low Temperatures. ASM International, OH, USA, 1997.
[11] C. Rubenstein. A general theory of the surface friction of solids. Proc. Phys. Soc. B69 (1956) 921-933.
[12] A. Nadai. Theory of flow and fracture of solids. McGraw-Hill Book Company, 1950.
[13] A.A. van der Stelt. Friction surface cladding, development of a solid state cladding process. PhD thesis, Universiteit Twente, 2014.
[14] J. Huétink, P.T. Vreede, J. van der Lugt, Progress in mixed Eulerian-Lagrangian finite element simulation of forming processes, Int. J. Num. Meth. Eng., 30, 1441-1457.
[15] E.A. El-Danaf. Mechanical properties and microstructure evolution of 1050 Aluminum severely deformed by ECAP to 16 passes. Mat. Sc. Eng. A487 (2008) 189-200.
[16] W.M. van Haaften, B. Magnin, W.H. Kool, L. Katgerman. Constitutive behaviour of as-cast AA1050, AA3104, and AA5182. Met. Mat. Trans. A33 (2002) 1971-1980.